

# Simplified evaluation of seismic behavior of beam-column joints in reinforced concrete frames



**G.P. Lignola, A. Prota & G. Manfredi**

*Department of Structural Engineering, University of Naples, Italy*

## **SUMMARY:**

A simplified analytical model of joint behaviour is discussed and theoretical simulations are performed in order to fully understand the seismic performance and the failure modes of beam-column joints in reinforced concrete buildings.

The rationale of the model is also to identify the strength hierarchy in terms of capacity for different failure modes (namely failure of the cracked joint, bond failure of the passing through bars, flexural/shear failures of beams or columns). The model focuses on both internal and external perimetric beam-column joints.

In this way this model results in a tool for the designer of new joints to quantify the performance of new structures, but also as a tool for the designer of external strengthening of existing joints in order to quantify the benefits of the operations and pushing the initial failure to a more desirable failure mode.

Further, some results of tests available in the scientific literature are reported, analysed and compared.

*Keywords: Beam-column joints, Analytical modelling, Capacity, Failure mode, Reinforced Concrete*

## **1. INTRODUCTION**

The behaviour of the beam-column joints is a crucial aspect in a Reinforced Concrete (RC) moment resisting frame and should be designed and detailed properly. Failure of beam-column joints during earthquakes is governed by bond and shear failure mechanisms which are brittle in nature. Beam-column joints having deficient reinforcement details are expected to respond poorly, even when subjected to moderate seismic action. Beam-column joints in a RC moment resisting frame are circumscribed portions of the structures where high loads transfer between the connecting elements (i.e. beams and columns) in the structure. This aspect can be particularly crucial especially in the case of seismic resistant frames where this high demand mobilizes the inelastic capacity of RC members to dissipate seismic energy while joints are poorly designed, jeopardizing the entire structure, even if it is correctly designed (Manfredi *et al.* 2008).

Under certain seismic actions, the beams connecting into a joint are subjected to moments in the same (clockwise or counter clockwise) direction. Under these moments, the bars at the same level are pulled or pushed in the same direction at both sides of the joint panel. If the column is not wide enough or if the strength of concrete in the joint is low, there is insufficient bond of the steel bars on concrete to balance this stress request (Lignola *et al.* 2010). In such cases, the reinforcement bars slip inside the joint region, and beams lose their load carrying capacity. Furthermore, under cyclic actions, joints undergo the diagonal push and pull actions and concrete diagonally cracks in the joint panel.

## **2. SIMPLIFIED MODELING OF INTERNAL AND EXTERNAL PERIMETRIC JOINTS**

The present work aims to provide a contribution to capacity design (and the subsequent strength hierarchy) principles. In fact these modern design principles are strongly subordinate to the beam-column joint panels' behaviour which can reduce substantially the global ductility, if the joint is

subjected to a premature failure. The analyses focus on two types of joints which can be identified in a perimeter moment resisting frame, namely interior joint and exterior joint. Perimeter frames are selected because they have less beneficial effect of confinement provided by out-of-plane members (i.e. transverse beams or slabs). Internal joints present two beams framing into the sides of a column, while external joints present a beam only framing into a side of corner columns.

Experimental joint failure databases (e.g. Kim 2007 collected data on 341 subassemblies) highlight typical shear failures in conjunction with, but also without, yielding of longitudinal beam reinforcement. Influencing parameters for joint shear behaviour are linked to key points on capacity curves displaying the most distinct stiffness changes. Concrete cracking is usually coupled to yielding or bond failure of longitudinal beam reinforcement when the most distinct changes in stiffness, for both overall and local behaviour, are triggered, up to the point of initiation of joint shear failure (maximum experimental storey shear).

The examined parameters for joint behaviour are: material property, joint panel geometry, reinforcement in joint panel, column axial load, reinforcement bond condition. Furthermore the effect of external strengthening, e.g. by means of externally bonded FRP, but not limited to it, is another parameter discussed in this paper. Obviously also shear and flexural capacity of intersecting elements, namely beams and columns, are of interest for the capacity design, hence they are considered herein but not analysed in details since they are considered almost well established, both in terms of as-built and strengthened capacity.

The proposed model moves from the so called quadruple flexural resistances model (Shiohara 2001) depicted in Fig. 2.1. It considers the kinematics of the four segments divided by diagonal cracks in joint panel, rotating due to bending moment and shear coming from beams and columns. The equilibrium of internal forces in steel and concrete and external forces acting on beam ends and column ends is taken into account, whereas the compatibility condition is not necessarily satisfied. Dowel effects of bars and shear friction along diagonal cracks are neglected, in the original formulation.

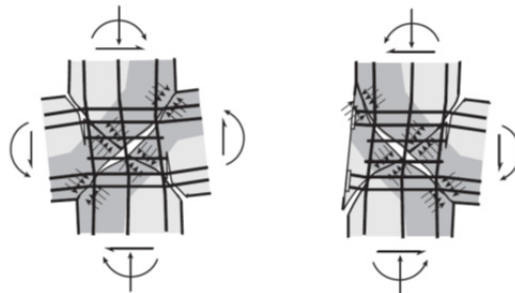


**Figure 2.1.**The basic scheme of original quadruple flexural resistance model (Shiohara 2001)

The model, as it was originally proposed, presents some essential assumptions, mainly because of undetermined system of equations having fewer equations than unknowns. For instance in the interior joint, accounting for symmetry, given 12 equations defining equilibrium (3 per rigid body), the number of independent equations representing the equilibrium reduces to 5. Conversely the unknowns are at least 8; so 3 of them were assumed equal to experimental recorded data in experimental validation or directly assigned in design phase. For instance yielding of joint stirrups is assumed (according to typical experimental outcomes after joint cracking) and also yielding of all beam bars, or alternatively yielding of tensile bars only and then the stress in compressed bars is derived by bond capacity limitation in the joint panel. The model was also split to analyse potential beam failure or joint failure (evidently, joint capacity is the smallest one of the two failure modes). However to avoid assuming many unknowns, either supplied by experimental outcomes or considered at their maximum capacity (e.g. steel at yielding point, which actually is not always yielded at joint failure looking at experimental databases), modified unknowns, different assumptions and solutions were proposed.

The basic idea is to include the beam mode into a unified joint model (adding apart a separate check not only of beam flexural failure, but also of column, and for both checking shear failure also). Doing so, it is possible to merge concrete compression and steel compression in a single compression force resultant at both beam and column ends. This assumption to merge compression in concrete and steel

reinforcement has almost no effect on equilibrium of beams, while has minor effect on columns where neutral axis is deeper (Cosenza *et al.* 2008). Finally, considering column shear not as an unknown, but as the main parameter to study the variability of all other internal force unknowns, it is possible to plot the evolution of such forces with shear column,  $V_c$ , and to match the number of equations and unknowns. In this way, according to basic capacity design principles, column shear capacity is provided for each failure mode (e.g. column shear corresponding to concrete compression failure, is found on the curve of concrete in compression at a  $V_c$  value intersecting concrete capacity; similarly  $V_c$  corresponding to bond failure is found on the bond demand curve intersecting bond capacity). The model is particularized for external and internal joints.

## 2.1. External perimetric joints

An external joint is depicted in Fig. 2.2. Main geometrical parameters are shown. Depth of beam,  $B_b$ , and column,  $B_c$ , can be different, being usually the depth of the joint,  $B$ , the minimum of the previous ones. Fig. 2.2 shows also force resultants in reinforcement bars,  $F_i$ , (e.g. for the depicted case of counter clockwise moments on beams and clockwise on columns,  $F_1, F_2, F_7$  and  $F_8$  are in compression, but a sign inversion is related to the sign of column shear,  $V_c$ ; similarly compression  $C$  moves on the other sides of the four blocks). Symbol  $\alpha$  is the ratio  $L_c/L_b$ , where the constraints of beams and columns are hinges representing contra flexure points (i.e. zero flexural moment).

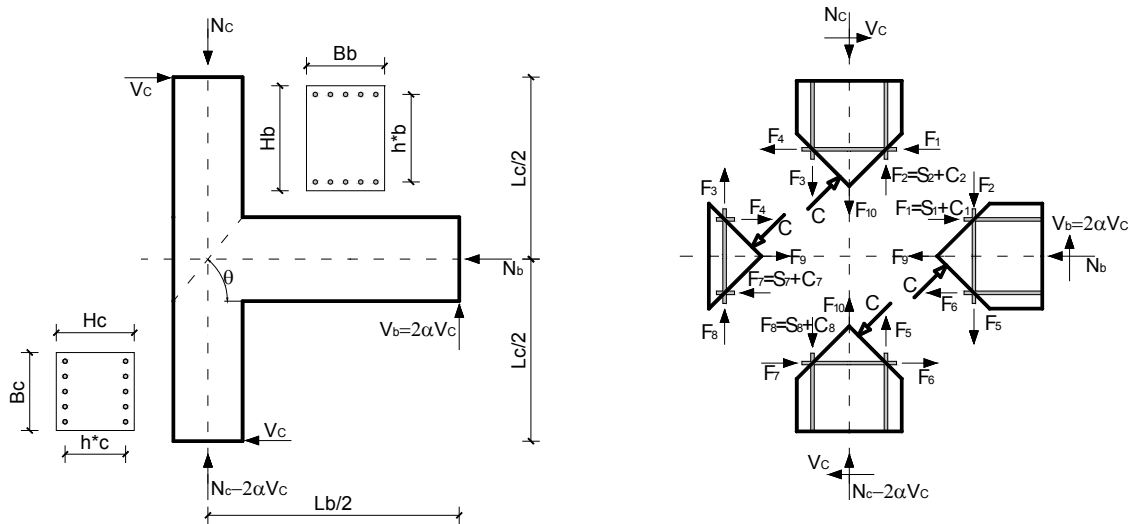


Figure 2.2. External perimetric joint: geometry, internal distribution of forces

It is noted that these  $F_i$  are force resultants and they are not strictly related to reinforcement cross-section or stresses (i.e. even if resultants are equal, bars can be different and also axial stress values inside each bar can be different). There is also explicitly the concrete contact force  $C$ , due to the compressed strut in the joint (see Fig. 2.1). For simplicity this force is assumed centred and inclined, angle  $\vartheta$ , equally to the diagonal of the joint panel, angle  $\theta$ , so that it is normal to the crack plane. However it can be inclined according to a different angle, to include also shear force transmission due to friction along the crack. Preliminary results indicate that increasing the angle  $\vartheta$ ,  $V_c$  joint capacity due to bond failure or shear failure, related to tensile yielding of beam bars, reduces. Conversely  $V_c$  joint capacity due to shear failure, related to tensile yielding of column bars, increases.

The concrete compression/contact forces at reinforcement level are incorporated in resultants  $F_1, F_2, F_7$  and  $F_8$  where reinforcement forces are  $S_1, S_2, S_7$  and  $S_8$ , while  $C_1, C_2, C_7$  and  $C_8$  represent horizontal and vertical components of concrete compression/contact forces. The nonlinear system in 9 unknowns ( $C, F_1, F_2, F_3, F_4, F_5, F_6, F_7$  and  $F_8$ ) follows:

$$F_1 + F_4 - C \sin \vartheta - V_c = 0 \quad (2.1a)$$

$$F_1 - F_6 - F_9 + C \sin \vartheta - N_b = 0 \quad (2.1b)$$

$$F_6 + F_7 - C \sin \vartheta - V_c = 0 \quad (2.1c)$$

$$F_2 - F_3 - F_{10} + C \cos \vartheta - N_c = 0 \quad (2.1d)$$

$$F_2 + F_5 - C \cos \vartheta - 2\alpha V_c = 0 \quad (2.1e)$$

$$F_8 - F_5 - F_{10} + C \cos \vartheta - N_c + 2\alpha V_c = 0 \quad (2.1f)$$

$$h_b^*(F_1 + F_4) + h_c^*(F_2 + F_3) - C^2/f_c B - L_c V_c = 0 \quad (2.1g)$$

$$h_b^*(F_1 + F_6) + h_c^*(F_2 + F_5) - C^2/f_c B - 2L_c V_c = 0 \quad (2.1h)$$

$$h_b^*(F_6 + F_7) + h_c^*(F_5 + F_8) - C^2/f_c B - L_c V_c = 0 \quad (2.1i)$$

All the unknowns are expressed as functions of column shear,  $V_c$ , and  $f_c$  is the mean concrete compressive strength. In this system,  $F_9$  and  $F_{10}$  represent the vertical and horizontal resultants of joint confinement systems (e.g. internal stirrups and/or externally bonded uni- or multi-axial FRP sheets) and are assumed to be known and equal to the capacity of the system (e.g. FRP debonding, considered as the maximum achievable capacity). Furthermore in this system  $V_c$  and beam shear,  $V_b$ , as well as flexural moment at column,  $M_c$ , or beam,  $M_b$ , interface with joint satisfy also these relations:

$$V_c = (V_b L_b)/(2L_c); \quad V_c = 2M_c/(L_c - Hb); \quad V_c = (M_b L_b)/[(L_b - Hc)L_c] \quad (2.2a; b; c)$$

It is highlighted that a sign inversion in column shear leads to a different equilibrium, however, due to length constraints, no specific figures and equations are provided, but the same approach should be followed. A higher axial load is expected on the lower column (i.e.  $N_c + 2\alpha V_c$  instead of  $N_c - 2\alpha V_c$ ); it has an impact on force resultant in tensile reinforcement and on shear and flexural capacity of the lower column, leading usually to more conservative results if beams and columns have symmetric reinforcements.

## 2.2. Internal joints

An internal joint is depicted in Fig. 2.3. Main geometrical parameters are shown. Fig. 2.3 shows force resultants,  $F_i$ , (e.g. for depicted case of clockwise moments on columns,  $F_1$  and  $F_2$  are in compression, but a sign inversion is expected and should be considered as in previous external joints). Symmetry is obvious if the joint is exactly at  $L_b/2$  and  $L_c/2$ , as it is usually in experimental and design schemes, however this does not mean that steel reinforcement bars having  $T_1$  as resultant force at bottom of right beam and at top of left beam have equal cross section or total area.

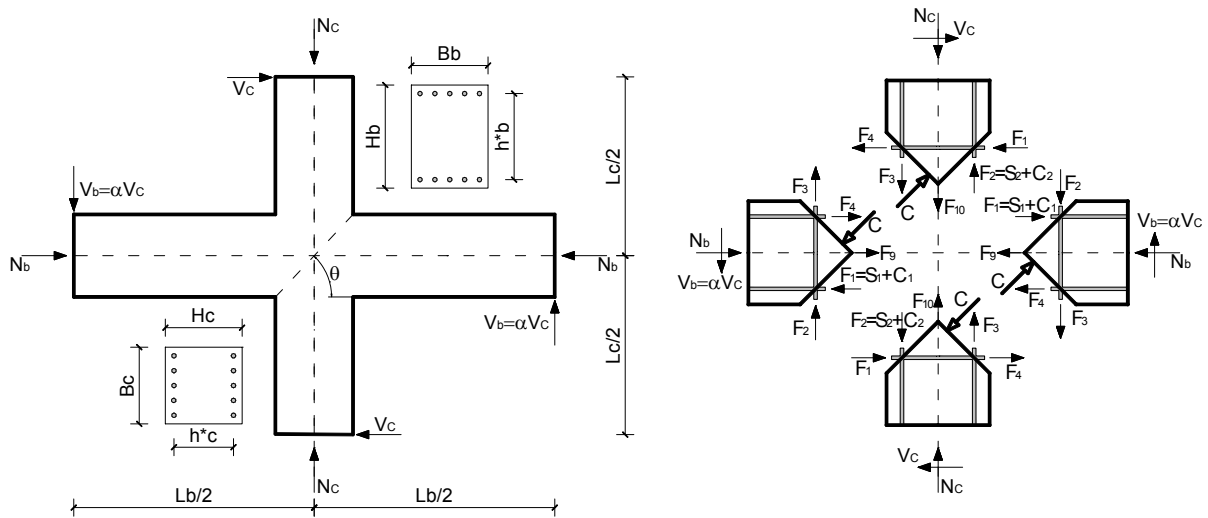


Figure 2.3. Internal perimetric joint: geometry, internal distribution of forces

Compared to previous case, this symmetry in terms of internal and external forces, but not necessarily in terms of reinforcement bars, reduces the number of nonlinear equations to 5, in 5 unknowns ( $C$ ,  $F_1$ ,  $F_2$ ,  $F_3$  and  $F_4$ ):

$$F_1 + F_4 - C \sin \vartheta - V_c = 0 \quad (2.3a)$$

$$F_1 - F_4 - F_9 + C \sin \vartheta - N_b = 0 \quad (2.3b)$$

$$F_2 - F_3 - F_{10} + C \cos \vartheta - N_c = 0 \quad (2.3c)$$

$$F_2 + F_3 - C \cos \vartheta - \alpha V_c = 0 \quad (2.3d)$$

$$h_b^* (F_1 + F_4) + h_c^* (F_2 + F_3) - C^2 / f_c B - L_c V_c = 0 \quad (2.3e)$$

In fact, compared to previous case,  $F_5=F_3$ ,  $F_6=F_4$ ,  $F_8=F_2$  and  $F_7=F_1$ . Furthermore in this system, column and beam shear,  $V_b$ , as well as flexural moment at column,  $M_c$ , or beam,  $M_b$ , interface with joint satisfy also these relations:

$$V_c = (V_b L_b) / (L_c); \quad V_c = 2M_c / (L_c - Hb); \quad V_c = 2(M_b L_b) / [(L_b - Hc)L_c] \quad (2.4a; b; c)$$

### 2.3. Failure modes

Paper focuses on joint failure; however, to fully understand joint behaviour, it is recommended to evaluate also beam and column peculiar failure modes (i.e. flexural and shear capacity, according to classical structural analysis approaches, Cosenza *et al.* 2008). These failure modes are expressed in terms of column shear according to Eqns. 2.2 or 2.4, thus providing the first four possible  $V_c$  capacity values corresponding to failure of the beam-column joint system.

Focusing on joint panel, three different failure modes can be expected: failure of concrete strut due to crushing, conventional failure due to yielding of longitudinal bars, bond failure of longitudinal bars (in fact, the joint panel has limited dimensions to anchor the high stress demand from bars).

The former failure mode involves the attainment of concrete crushing in the diagonal strut, so  $C$  should be limited to

$$C_{\max} = B \cdot f_c \cdot Hb / (2 \sin \theta) \quad (2.5)$$

If the force  $C$  was assumed inclined not as the diagonal (i.e.  $\vartheta \neq \theta$ ), a shear friction check should be also performed. Afterwards, conventional failure of reinforcement in tension is checked, assuming different bars at each longitudinal reinforcement level  $i$ , having cross section  $A_k$  and yielding stress  $f_{y,k}$ .

So each  $F_i$  should be limited to:

$$F_{\max,i} = \sum A_k f_{y,k} \quad (2.6)$$

Finally the latter failure mode requires to split compression resultant force into steel and concrete contributions (Fig. 2.4).

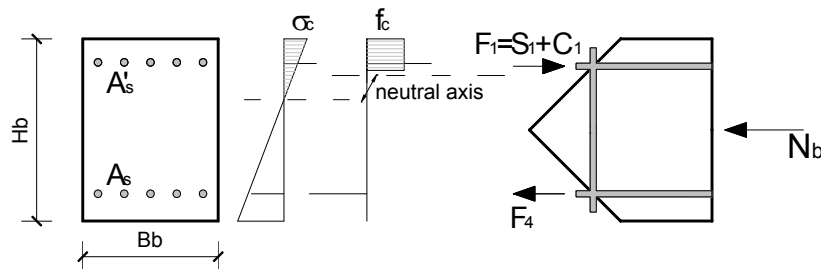


**Figure 2.4.** Analysis of distribution of compressive forces in concrete and reinforcement

The basic idea is to evaluate (according to classical structural analysis approaches, Cosenza *et al.* 2008) the neutral axis depth, recalling linearity of strain diagram of cross section; in the meantime compression and tensile resultants are in equilibrium, according to previous systems of equations. Fig. 2.4 remembers also that neutral axis changes with increasing flexural loads. The neutral axis,  $c$ , can be evaluated, for instance in the elastic field in a beam, without axial load, equating first order moment to zero (Eqn. 2.7a) and, once  $c$  is known,  $S_1$  is derived:

$$Bb \cdot c^2 + n \left[ A'_s (2c - Hb + h_b^*) - A_s (Hb + h_b^* - 2c) \right] = 0 \quad (2.7a)$$

$$S_1 = F_4 \frac{A'_s (2c - Hb + h_b^*)}{A_s (Hb + h_b^* - 2c)} \quad (2.7b)$$

Finally, computing effective bond length,  $L_{eb}$ , the upper bound bond capacity of concrete (based on uniform bond stress capacity  $\tau$ ) is compared to the bond demand, given by the anchoring of longitudinal bars, even with different diameter  $\Phi_k$ , at the same level, e.g. due to two resultants  $S_1 + F_4$ :

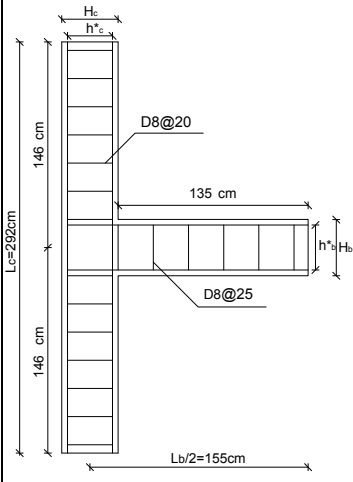
$$L_{eb} = h_b^* / tg\theta; \quad (S_1 + F_4)_{\max} = \tau \sum L_{eb,k} \Phi_k \quad (2.8a; b)$$

Three different bond stress capacities were considered according to Model Code 90 (CEB-FIP Model Code, 1990): the bond capacity,  $\tau_{\max}$ , is equal to  $2.5\sqrt{f_c}$  (good bond) or  $\tau_{\text{med}}=1.25\sqrt{f_c}$  (all others conditions) for ribbed bars. A further value,  $\tau_{\min}$ , of  $0.3\sqrt{f_c}$  can be used in the case of smooth bars. However it is highlighted that, especially in external joints, specific anchorage solutions can be adopted. They are out of the scope of present work, however they can be evaluated and inserted in the proposed model as bond capacity threshold, e.g.  $(S_1 + F_4)_{\max}$ , to estimate corresponding  $V_c$ .

### 3. BEHAVIOR OF PROPOSED SIMPLIFIED MODEL

To evaluate the behaviour of proposed simplified model, a parametric analysis is performed, in particular on an external perimetric joint, to highlight peculiarities of this joint, lacking of symmetry simplifications, unlike internal joints. Main parameters were: axial load on column,  $N_c$ ; concrete strength,  $f_c$ ; stirrups in the joint; FRP externally bonded on the joint panel; longitudinal reinforcement ratio in beams and columns; beam height, hence joint panel dimensions. Their variability is depicted in the following numerical test matrix (table 3.1).

**Table 3.1.** Numerical test matrix of parametric analysis

	ID	$N_c$ [kN]	$f_c$ [MPa]	Stirrups	FRP	Reinf.	$H_b$ [cm]	Failure mode and $V_c$ [kN]
		1	0	20	n.a.	n.a.	min	40
	2	200	(J) 18.44					
	3	400	(J) 18.44					
	4	200	40	2D8 <sub>2legs</sub>	n.a.	min	40	(J) 18.53
	5		60					(J) 18.57
	6		20					n.a.
	7	1 ply		(J) 21.25				
	8	1 ply*		(BF) 21.50				
	9	200	20	n.a.	2 plies	min	40	(BF) 21.50
	10							(BS) 77.77
	11							(J) 44.20
	12				n.a.	max	60	
						min	60	

FRP is quadriaxial and ply thickness is 0.053 mm; \*is uniaxial FRP; (J) is joint failure due to beam tensile reinforcement yielding; (BF) is beam flexural failure; (BS) is beam shear failure; min reinf. calls for 3+3D12 in beams and 3+3D14 in columns; max reinforcement calls for 6+6D32 in beams and columns;  $f_y=450$  MPa,  $B=30$  cm,  $H_c=40$  cm, 4 cm cover;

The 12 analyses allow to assess the influence of different parameters, both in terms of failure mode and of column shear,  $V_c$ . In some cases, a parameter has no influence on the effective failure mode, however it has an influence on other possible failure modes, but not triggered first in that case. The effect of axial load is mainly on column reinforcement forces and flexural and shear capacity (see Fig. 3.1a where the force resultant  $F_1$  reaches its yielding value at increasing column shear,  $V_c$ , when increasing  $N_c$ ). In Fig. 3.1a  $F_3(V_c)$  curves have different origin because the higher is the axial load, the higher is initial compression level at zero lateral load,  $V_c$ . Similarly column shear corresponding to column flexural failure changes from 59.0 kN to 110.5 kN, yet being not triggered as first failure mode. Axial load has negligible effect on joint failure. The effect of concrete strength is related mainly to shear and flexural capacity of beams and columns, e.g.  $V_c$  corresponding to column flexural failure changes from 85.1 kN to 91.6 kN;  $V_c$  corresponding to beam flexural failure changes from 21.5 kN to 23.6 kN, being not triggered as first failure mode. A clear effect is also on bond capacity; Fig. 3.1b shows bond demand  $F_6+S_7$  reaching its capacity value at increasing  $V_c$ , when changing  $\tau_{\max}(f_c)$ .

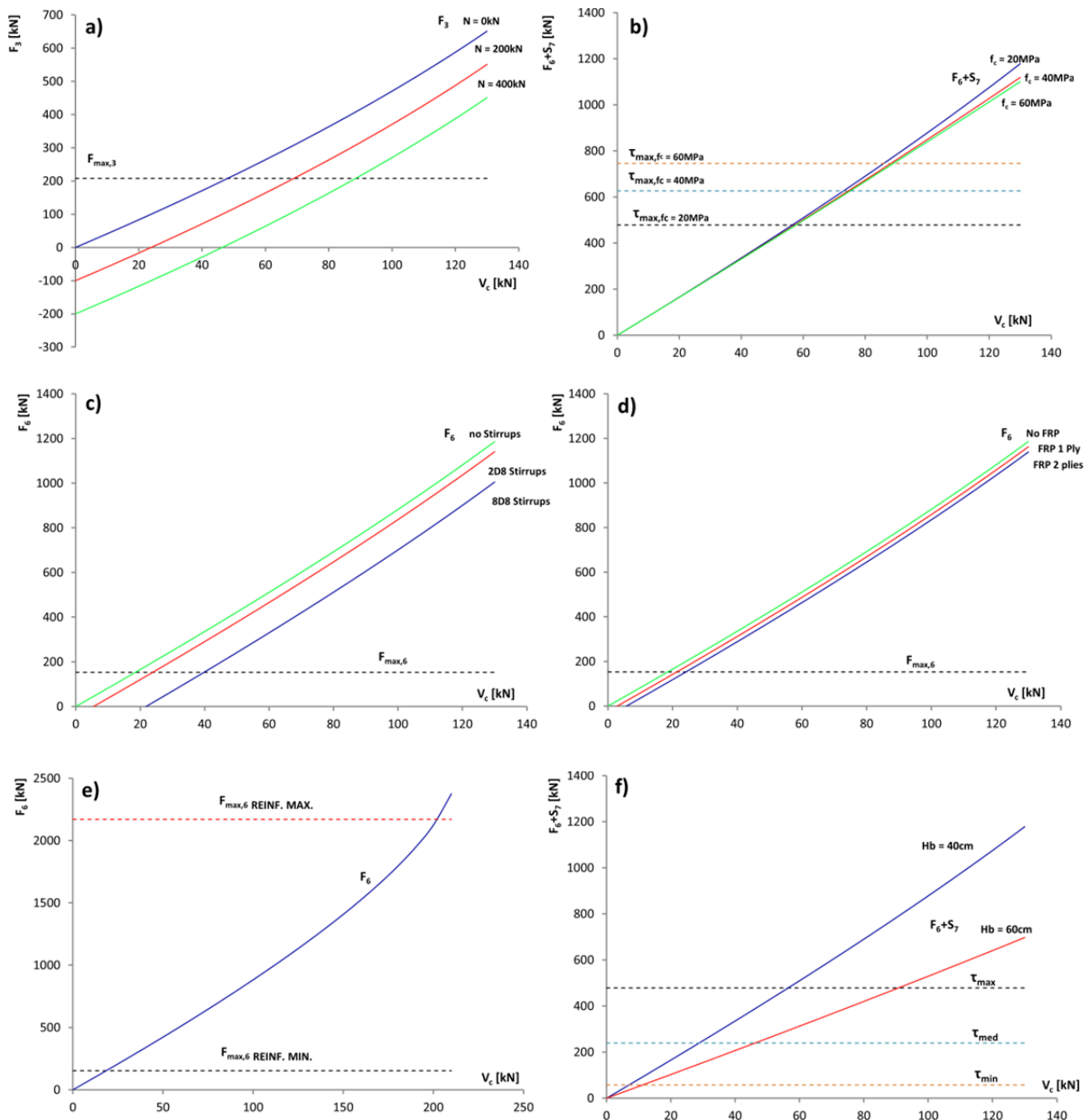


**Figure 3.1.** Parametric analysis highlighting: a) variability of axial load  $N_c$ , b) variability of concrete strength  $f_c$ , c) variability of stirrups, d) variability of externally bonded FRP, e) variability of longitudinal beam reinforcement, f) variability of beam height, hence of joint panel dimensions

Concrete strength has also negligible influence on application point of C, leading to slight changes in joint shear capacity (in present case actual failure is due to beam tensile reinforcement yielding). The effect of stirrups is meaningful, it has many consequences. The most relevant is on longitudinal reinforcement bars, reducing their load, thus bearing a portion of horizontal load demand. Stirrups are assumed to yield, and for simplicity, their tensile force ( $T_9$ ) is assumed equal to yielding force from the very beginning; for this reason, in Fig. 3.1c the  $F_6(V_c)$  curves have different origin. However the presence of stirrups increases column shear corresponding to joint failure due to beam tensile reinforcement yielding from 18.4 kN (no stirrups and actual failure of #2 analysis) to 23.8 kN (two D8 stirrups with two legs) and 39.8 kN (eight D8 stirrups with two legs), but in these cases failure mode switches to beam flexural failure. So it can be concluded that, in this case, two D8 stirrups are enough to change the failure mode from brittle joint failure to most desirable ductile beam flexural failure. Similar comments can be repeated for FRP externally bonded. The role of the reinforcement is similar to the insertion of stirrups, however benefits can be achieved also on existing joint, even if originally they have no internal stirrups. From a numerical point of view, the presence of FRP is similar to stirrups; both provide an increase of horizontal,  $T_9$ , (or vertical,  $T_{10}$ , if vertical fibers are also applied) load carrying capacity. FRP strain is assumed equal to debonding value (e.g. 0.4% according to Italian guidelines CNR DT200 2004), and FRP tensile force is assumed equal to debonding force from the very beginning. For this reason, in Fig. 3.1d the  $F_6(V_c)$  curves have different origin. However the presence of FRP increases  $V_c$  value, corresponding to system failure, from 21.2 kN (yet joint failure due to beam tensile reinforcement yielding) to 23.5 kN (two plies of quadriaxial FRP). FRP was able to change the failure mode from brittle joint failure to most desirable ductile beam flexural failure. Longitudinal reinforcement has no influence on the evaluation of resultants, e.g. Fig. 3.1e shows the  $F_6(V_c)$  curves, they overlap, however the yielding capacity is different thus leading to much different  $V_c$  values, corresponding to beam tensile reinforcement yielding. These  $V_c$  values increase from 18.4 kN (actual failure of #2 analysis) to 202.2 kN (high reinforcement ratio), however the first triggered failure mode is beam shear, at a lower  $V_c=77.7$  kN. It is not a desired failure mode, due to its brittleness. However it is a well-known outcome: when increasing too much reinforcement ratio, flexural capacity increases, but this may lead to unbalanced shear capacity, thus switching to a less desirable brittle shear failure. Similarly the increase of beam dimensions has two main effects: the first one is the increase of beam capacity, both in terms of flexure and shear; the second one is the increase of joint panel dimensions. The increase of joint panel dimensions reduces the demand in terms of force resultant in reinforcements, as shown in Fig. 3.1f where the bond demand is clearly lower for the higher beam. The same figure highlights also the influence of bond capacity: the same beam-column joint, if reinforced with smooth bars presents a much lower capacity. In the case of 60x30 beams, potential failure due to bond occurs at 90.7 kN in the case of good bond for ribbed bars, and it drops dramatically to 11.2 kN in the case of smooth bars. It is a “potential” failure mode in the case of good bond with ribbed bars, because the actual failure mode is joint shear due to longitudinal tensile reinforcement yielding at  $V_c=44.2$  kN. Compared to counterpart analysis #2 (differing only for beam height), the increase of joint panel dimensions increases the failure load. Conversely if smooth bars were used, predicted failure mode of the system would have occurred due to bond failure at a very low value  $V_c=11.2$  kN. This let to conclude that bond capacity has a meaningful effect on beam-column joint strength.

#### 4. THEORETICAL/EXPERIMENTAL COMPARISONS

Predictions of proposed simplified model were also compared to some experimental tests available in literature (El-Amoury and Ghobarah 2002, Masi and Santarsiero 2008, Russo and Pauletta 2012 for external perimeteric joints and Zaid et al. 1999, Hakuto et al. 1999, Prota et al. 2004 for internal perimeteric joints). Only one beam-column joint specimen is discussed in detail showing the entire table of failure modes (see table 4.1). Actual failure load is the smallest one of the potential failure modes. This approach allows not only to better understand the strength hierarchy, but also to calibrate strengthening design.

The basic idea is to avoid all undesired failure modes (e.g. brittle shear failure of joint, but also of

beams and columns) to push failure mode to more desirable ductile beam flexural failure. Once the desired failure mode is selected, than all failure mode mechanisms presenting lower column shear values should be improved and strengthenings (on existing structures) or design improvements (in structures still under design) can be calibrated to exceed the  $V_c$  corresponding to desired failure mode (i.e. according to classical capacity design approach).

A test by Masi and Santarsiero 2008 showed the peculiarity of beam longitudinal bar breaking and for this reason the model predictions included not only the yielding of longitudinal beam reinforcement, but also the failure of bars occurring at a ultimate stress about 23% higher than yielding. This is reflected by the first triggered failure mode that is related to longitudinal bars, but, compared to bar yielding at  $V_c=13.6$  kN, bar breaking occurred at  $V_c=16.7$  kN. Experimental failure occurred at 18 kN, being the scatter about 7%. Table 4.1 shows that shear failure due to beam longitudinal bar yielding is almost close to flexural failure of beam, so that a slight strengthening of this joint panel is required to move from undesired brittle joint shear failure to desired ductile flexural failure of beams. Next figure shows main geometrical dimensions; axial load on column was  $N_c=290$  kN, while concrete compressive strength was 17.8 MPa and steel yielding stress was 478 MPa. Table 4.1 remarks again the crucial influence of bond capacity on the performance of such systems; smooth bars, providing reduced bond performance (neglecting specific anchoring solutions), reduce the column shear,  $V_c$ , ultimate capacity to about 3 kN.

**Table 4.1.**Detailed predictions of simplified model for Masi and Santarsiero 2008 experimental test, #T1

Failure mode	$V_c$ [kN]
Beam flexure	17.75
Column flexure	56.46
Beam shear	156.78
Column shear	145.89
Crushing of diagonal strut	99.18
Tensile yielding, beam bars	13.59
Tensile yielding, upper column bars	86.40
Tensile yielding, lower column bars	74.70
Bond (good bond, $\tau_{max}$ )	25.62
Bond (ribbed bars, $\tau_{med}$ )	13.00
Bond (smooth bars, $\tau_{min}$ )	3.15

For the other experimental tests (whose basic data are not repeated from corresponding references due to length constraints), the actual experimental failure mode and load, and the predicted failure mode and load are compared in table 4.2 and table 4.3. Maximum percentage difference in terms of failure load is about 15% and also failure modes are almost satisfactorily predicted.

**Table 4.2.**General comparison of experimental outcomes and simplified model predictions: external joints

Reference and Specimen ID	Experimental		Theoretical		Difference %
	Failure mode	$V_c$ [kN]	Failure mode	$V_c$ [kN]	
El-Amoury and Ghobarah(2002) T0	J	58.5	J	59.1	+1%
Masi and Santarsiero (2008) T1	BB	18.0	BB	15.9	-12%
Masi and Santarsiero (2008) T5	J	43.0	J	43.6	+2%
Russo and Pauletta (2012) 12-6+	J	6.8	J	7.5	+10%
Russo and Pauletta (2012) 12-6-	B	3.17	B	2.9	-9%
Russo and Pauletta (2012) 12-8	J	8.18	J	8.3	+2%
Russo and Pauletta (2012) 16-6	J	7.36	J	8.5	+15%

(J) is joint failure due to beam tensile reinforcement yielding; (B) is bond failure; (BB) is tensile breaking of beam bars

**Table 4.3.** General comparison of experimental outcomes and simplified model predictions: internal joints

Reference and Specimen ID	Experimental		Theoretical		Difference %
	Failure mode	V <sub>c</sub> [kN]	Failure mode	V <sub>c</sub> [kN]	
Zaid et al. (1999) S3	J	130.0	J	121.5	-6%
Hakuto et al. (1999) O1	J	89.0	J	76.1	-14%
Hakuto et al. (1999) O5	BS	150.0	J	137.1	-9%
Prota et al. (2004) L1	CF	32.7	CF	31.2	-5%
Prota et al. (2004) H1	CF	37.7	J	32.2	-14%
Prota et al. (2004) L2	CF	31.6	CF	33.3	+5%
Prota et al. (2004) H2	J	38.4	J	32.9	-14%

(J) is joint failure due to beam tensile reinforcement yielding; (CF) is column flexural failure; (BS) is beam shear failure

## 5. CONCLUDING REMARKS

The beam-column joints behaviour can strongly influence the seismic performance of RC buildings. A simplified analytical/mechanical model of joint behaviour is discussed and theoretical simulations are performed in order to fully understand the mechanical behaviour and the failure modes.

The model moves from a previous one, but it improves and alters deeply the main unknowns, assumptions and solutions. Among main parameters affecting the performance of joints, namely material property, joint panel geometry, reinforcement in joint panel, column axial load, reinforcement bond condition; axial load on columns showed negligible influence, while meaningful influence was given by bond performance. Similarly, joint (transverse) reinforcement, either external FRP or internal stirrups, provides many benefits pushing failure mode from brittle joint shear to ductile beam flexural.

## ACKNOWLEDGEMENTS

The authors acknowledge the financial support provided by ReLUIS for the research program funded by the Department of Civil Protection – Executive Project 2010-2013.

## REFERENCES

- CEB-FIP Model Code (1990). “Design Code”. Comité Euro-International du Béton. Thomas Telford.
- CNR-DT 200 (2004). Guide for the Design and Construction of Externally Bonded FRP Systems for Strengthening Existing Structures. National Research Council, Roma, Italy.
- Cosenza, E., Manfredi G. and Pecce M. (2008). Strutture in cemento armato: Basi della progettazione. HOEPLI, Italy. *In Italian*.
- El-Amoury, T., and Ghobarah, A. (2002). Seismic rehabilitation of beam-column joint using GFRP sheets. *Engineering Structures*, **24**, 1397–1407.
- Hakuto, S., Park, R., Tanaka, H. (1999). Effect of deterioration of bond of beam bars passing through interior beam-column joints on flexural strength and ductility. *ACI Structural Journal*, **96:5**, 858-864.
- Kim, J. (2007). Joint Shear Behavior of Reinforced Concrete Beam-column Connections Subjected to Seismic Lateral Loading, Ph.D. Thesis at University of Illinois at Urbana-Champaign, ProQuest LLC, (MI), USA
- Lignola, G.P., Verderame, G.M. and Manfredi, G. (2010). Effect of bond on seismic performance of internal joints in reinforced concrete frames. *14th European Conference on Earthquake Engineering*. Paper ID 640
- Manfredi, G., Verderame, G.M. and Lignola, G.P. (2008). A F.E.M. Model For The Evaluation Of The Seismic Behavior Of Internal Joints In Reinforced Concrete Frames. *14th World Conference on Earthquake Engineering*. Paper ID:05-01-0189
- Masi, A. and Santarsiero, G. (2008). Sperimentazione su nodi trave-colonna in c.a. progettati con diversi livelli di protezione sismica: primi risultati. Valutazione e riduzione della vulnerabilità sismica di edifici esistenti in c.a. ReLUIS, Roma: 521-529. *In Italian*.
- Prota A., Nanni A., Manfredi G., Cosenza E. (2004). Selective Upgrade of Underdesigned Reinforced Concrete Beam-Column Joints Using Carbon Fiber-Reinforced Polymers. *ACI Structural Journal* **101:5**, 699-707.
- Russo, G. and Pauletta, M. (2012). Seismic Behavior of exterior beam-column connections with plain bars and effects of upgrade. *ACI Structural Journal* **109:2**, 225-233
- Shiohara H. (2001). “New Model for Shear Failure of RC Interior Beam-Column Connections”. *ASCE J. Struct. Engrg.*, **127:2**, 152-160
- Zaid, S., Shiohara, H., Otani, S. (1999). Test of a joint reinforcing detail improving joint capacity of r/c interior beam-column joint. *1st Japan-Korea Joint Seminar on Earthquake Engineering for Building Structures*, Seoul National University, Seoul, Korea